Results

Interaction between epithelial and mesenchymal cells is important for tooth development. This interaction is mediated by the ECM, which acts as a cytokine store *in vivo*. It is therefore important to mimic ECM functions when constructing an *in vitro* co-culture system. We constructed two co-culture models to investigate the interaction between two different dental cell lines, a rat HAT-7 cell line that originated from dental epithelia, and bovine BCPb8 cells, derived from cementoblast progenitor cells (Fig. 1). One co-culture method, (sandwich co-culture; SW) cultured these cells by inoculation of the cell lines onto opposite sides of a collagen film suspended in a cell culture dish. The second, control method, termed "separate co-culture" (SC) cultured BCPb8 cells on the culture dish and the HAT-7 cells on a collagen film that faced away from the BCP8 cells on the dish.

To determine the gene expression levels of enamel matrix proteins quantitatively, we performed real-time PCR analysis using specific primers (Kurosawa et al. 2005). The specific rat primers used for this analysis were designed from regions of low-homology between rat and bovine cDNA to avoid cross-amplification. Glyceraldehyde-3-phosphate dehydrogenase mRNA expression in each cell line was used as an internal control. Ameloblastin mRNA expression in these culture systems is shown in Fig. 2. In the SW cells, the expression level of ameloblastin mRNA gradually increased after seeding of HAT-7 cells and continued to increase until at least day 14. The ameloblastin expression level was significantly increased on day 14 compared with the others condition such as SC culture, monolayer culture on a collagen membrane (ML). The degree of ameloblastin mRNA up-regulation in SC-cultured cells was less than that of SW-cultured cells on days 7 and 14. These results suggested that direct

interaction of HAT-7 and BCPb8 via the collagen membrane was important for tooth differentiation.

The expression of amelogenin mRNA in these culture systems is shown in Fig. 3. In the SW cells, the expression levels of amelogenin mRNA gradually increased after seeding of HAT-7 cells and continued to increase until at least day 14. On day 14, amelogenin expression was increased compared to HAT-7 cells grown in either monolayer culture or in SC method, although the difference compared to either control culture was not statistically significant. These results further suggest that direct interaction of HAT-7 and BCPb8 cells via a collagen membrane was important for tooth differentiation.

We next analyzed expression of the ameloblastin protein in the SW system by immunofluorescent staining using an anti-ameloblastin antibody, an Alexa 488-conjugated second antibody, and confocal laser scanning microscopy. The Alex488-Ameloblastin signal was detected in sandwich co-cultured HAT-7 cells from 3 days and had disappeared by day 14 (Fig. 4B, C and D). No ameloblastin signal was detected on day 1 of culture (Fig.4A). Ameloblastin protein expression was not detected in co-cultured BCPb8 cells on day 14 (Fig. 4E). These results indicate that HAT-7 cells can gradually differentiate into ameloblast-like cells in the SW system but not in the SC. These results suggest that interaction between HAT-7 and BCPb8 cells via a collagen membrane was important for tooth differentiation in protein expression level.

Discussion

We constructed and compared two *in vitro* culture systems both of which involved culture using a collagen membrane. Whereas, in both co-culture systems the two cell lines are exposed to soluble factors produced by both cell lines, only the SW co-culture system allows the two cell lines to physically contact each other through the collagen membrane. Our results showed that both the mRNA and protein expression of the ameloblastin were significantly increased in HAT-7 cells that were co-cultured with BCPb8 cells using the SW method. Soluble factors produced by the BCPb8 cells may also contribute to induction of ameloblastin expression. Furthermore, our data indicated that the collagen membrane might play a role, not only in the accumulation of, but also in the stabilization of, soluble factors from BCPb8 cells.

Although the soluble factors produced by BCPb8 cells that contribute to amelogenin expression have not been studied, they must be of relatively low molecular weight since only molecules with a molecular weight of less than 12.5 kDa can pass through the collagen membrane. Several soluble factors are known to be involved in the interaction between epithelial and mesenchymal tissue during tooth development including growth factors, cytokines and extracellular matrix molecules. Among these factors, the insulin-like growth factors (IGFs) have been proposed as autocrine/paracrine regulators of in vivo tooth development (Caton et al. 2005; Yamamoto et al. 2006) and the molecular weight of IGF is less than 12.5 kDa. Therefore, IGFs are promising candidate soluble factors for mediation of the stimulation of ameloblastin mRNA and protein expression in HAT-7 cells.

We reconstructed the interaction of dental epithelial and mesenchymal cells by co-culture of these cells using a collagen membrane *in vitro.* This method is easier to

perform than other methods of co-culture that use extracellular matrix components such as Matrigel. Using this method we were able to analyze cell signal transduction pathways that require dental epithelial and mesenchymal cell interactions. This study provides a useful tool for future analysis of epithelial-mesenchymal interactions.

Acknowledgments

This research was partially supported by the grant program "Collaborative Development of Innovative Seeds" from the Japan Science and Technology Agency (JST).

References

Aberg T, Wozney J, Thesleff I. 1997. Expression patterns of bone morphogenetic proteins (Bmps) in the developing mouse tooth suggest roles in morphogenesis and cell differentiation. Dev Dyn 210(4):383-96.

Caton J, Bringas P, Jr., Zeichner-David M. 2005. IGFs increase enamel formation by inducing expression of enamel mineralizing specific genes. Arch Oral Biol 50(2):123-9.

Cerny R, Slaby I, Hammarstrom L, Wurtz T. 1996. A novel gene expressed in rat ameloblasts codes for proteins with cell binding domains. J Bone Miner Res 11(7):883-91.

Fong CD, Slaby I, Hammarstrom L. 1996. Amelin: an enamel-related protein, transcribed in the cells of epithelial root sheath. J Bone Miner Res 11(7):892-8.

Fukumoto S, Kiba T, Hall B, Iehara N, Nakamura T, Longenecker G, Krebsbach PH, Nanci A, Kulkarni AB, Yamada Y. 2004. Ameloblastin is a cell adhesion molecule required for maintaining the differentiation state of ameloblasts. J Cell Biol 167(5):973-83.

Gingras M, Bergeron J, Dery J, Durham HD, Berthod F. 2003. In vitro development of a tissue-engineered model of peripheral nerve regeneration to study neurite growth. Faseb J 17(14):2124-6.

Hu CC, Fukae M, Uchida T, Qian Q, Zhang CH, Ryu OH, Tanabe T, Yamakoshi Y, Murakami C, Dohi N and others. 1997. Sheathlin: cloning, cDNA/polypeptide sequences, and immunolocalization of porcine enamel sheath proteins. J Dent Res 76(2):648-57.

Jernvall J, Keranen SV, Thesleff I. 2000. Evolutionary modification of development in mammalian teeth: quantifying gene expression patterns and topography. Proc Natl Acad Sci U S A 97(26):14444-8.

Kawano S, Morotomi T, Toyono T, Nakamura N, Uchida T, Ohishi M, Toyoshima K, Harada H. 2002. Establishment of dental epithelial cell line (HAT-7) and the cell differentiation dependent on Notch signaling pathway. Connect Tissue Res 43(2-3):409-12.

Krebsbach PH, Lee SK, Matsuki Y, Kozak CA, Yamada KM, Yamada Y. 1996. Full-length sequence, localization, and chromosomal mapping of ameloblastin. A novel tooth-specific gene. J Biol Chem 271(8):4431-5.

Kurosawa Y, Taniguchi A, Okano T. 2005. Novel method to examine hepatocyte-specific gene expression in a functional coculture system. Tissue Eng 11(11-12):1650-7.

Ohno M, Motojima K, Okano T, Taniguchi A. 2008. Up-regulation of drug-metabolizing enzyme genes in layered co-culture of a human liver cell line and endothelial cells. Tissue Eng Part A 14(11):1861-9.

Orisaka M, Mizutani T, Tajima K, Orisaka S, Shukunami K, Miyamoto K, Kotsuji F. 2006. Effects of ovarian theca cells on granulosa cell differentiation during gonadotropin-independent follicular growth in

cattle. Mol Reprod Dev 73(6):737-44.
Saito M, Handa K, Kiyono T, Hattori S, Yokoi T, Tsubakimoto T, Harada H, Noguchi T, Toyoda M, Sato S and others. 2005. Immortalization of cementoblast progenitor cells with Bmi-1 and TERT. J Bone Miner Res 20(1):50-7.
Smith CE. 1998. Cellular and chemical events during enamel maturation. Crit Rev Oral Biol Med 9(2):128-61.
Takayama G, Taniguchi A, Okano T. 2007. Identification of differentially expressed genes in hepatocyte/endothelial cell co-culture system. Tissue Eng 13(1):159-66.
Takezawa T, Nitani A, Shimo-Oka T, Takayama Y. 2007. A protein-permeable scaffold of a collagen vitrigel membrane useful for reconstructing crosstalk models between two different cell types. Cells Tissues Organs 185(1-3):237-41.
Thesleff I, Hurmerinta K. 1981. Tissue interactions in tooth development. Differentiation 18(2):75-88.
Thesleff I, Mikkola M. 2002. The role of growth factors in tooth development. Int Rev Cytol 217:93-135.
Thesleff I, Sharpe P. 1997. Signalling networks regulating dental development. Mech Dev 67(2):111-23.
Velazquez OC, Snyder R, Liu ZJ, Fairman RM, Herlyn M. 2002. Fibroblast-dependent differentiation of human microvascular endothelial cells into capillary-like 3-dimensional networks. Faseb J 16(10):1316-8.
Xu L, Harada H, Taniguchi A. 2006a. The exon 6ABC region of amelogenin mRNA contribute to increased levels of amelogenin mRNA through amelogenin protein-enhanced mRNA stabilization. J Biol Chem 281(43):32439-44.
Xu L, Harada H, Yokohama-Tamaki T, Matsumoto S, Tanaka J, Taniguchi A. 2006b. Reuptake of extracellular amelogenin by dental epithelial cells results in increased levels of amelogenin mRNA through enhanced mRNA stabilization. J Biol Chem 281(4):2257-62.
Yamamoto T, Oida S, Inage T. 2006. Gene expression and localization of insulin-like growth factors and their receptors throughout amelogenesis in rat incisors. J Histochem Cytochem 54(2):243-52.

Figure legends

Figure 1. Construction of the *in vitro* dental cell co-culture systems.

Two dental cell lines were co-cultured in *in vitro* co-culture systems using a transparent collagen membrane. The two cell lines used were: a dental epithelial cell line (HAT-7) established from a cervical loop epithelium of a rat incisor, and a dental follicle cell line (BCPb8) established from the follicle tissue of a bovine incisor. The Sandwich co-culture (SW) method involved inoculation of HAT-7 cells into one side of a collagen film suspended in a culture dish, and inoculation of BCPb8 cells onto the opposite side of the same collagen film (B). The separate co-culture method (SC) involved seeding of BCPb8 cells onto a cell culture dish, followed by seeding of HAT-7 cells onto a collagen film in the same a dish, using the side of the film facing away from the BCPb8 cells (A)."

Figure 2. Sandwich co-culture of HAT-7 cells enhances Ameloblastin mRNA expression. The level of ameloblastin mRNA expression in HAT-7 cells grown in monolayer culture on a collagen membrane (white bars; ML), in the sandwich co-culture system (black bars; SW), or in the separate co-culture system (grey bars; SC) was analyzed. Total RNA was prepared from the cells at the indicated time points and was used for the synthesis of cDNA. The levels of ameloblastin mRNA expression were analyzed using real-time PCR and species-specific primers. Data were normalized to glyceraldehyde-3-phosphate dehydrogenase (GAPDH) mRNA expression levels in the same sample. Values are presented as means ± standard deviation (n=3). Error bars indicate the standard deviation of mean changes. Data were statistically analyzed using student t test. *$p<0.05$

Figure 3. Sandwich co-culture of HAT-7 cells enhances Amelogenin mRNA expression. The level of amelogenin mRNA expression in HAT-7 cells grown in monolayer culture on a transparent collagen membrane (white bars; ML), in the sandwich co-culture system (black bars; SW) or in the separate co-culture system (grey bars; SC) was analyzed. Total RNA was prepared from the cells at the indicated time points and was used for synthesis of cDNA. The levels of amelogenin mRNA expression were analyzed using real-time PCR and species-specific primers. Data were normalized to glyceraldehyde-3-phosphate.dehydrogenase (GAPDH) mRNA expression levels in the same sample. Values are presented as means ± standard deviation (n=3). Error bars indicate the standard deviation of mean changes. Data were statistically analyzed using student t test. *$p<0.05$

Figure 4. Sandwich co-culture of HAT-7 cells enhances Ameloblastin protein expression. Ameloblastin protein expression in sandwich co-cultured HAT-7 and BCPb8 cells was analyzed on days 1 (A), 3 (B), 7 (C) and 14 (D and E) of culture using immunofluorescence. On each day, HAT-7 cells were fixed and stained for ameloblastin (green) and nuclei were stained with Hoechst 33258 (blue). The cells were analyzed using a confocal laser scanning microscope. The image in E is a cross-sectional view of the 14 days sample. Ameloblastin protein expression was detected in HAT-7 cells (arrow in E) but not in BCPb8 cells (D). The expression of ameloblastin protein was detected in HAT-7 cells from day 3 of the sandwich co-culture with BCPb8 cells.

(A)

A transparent collagen membrane

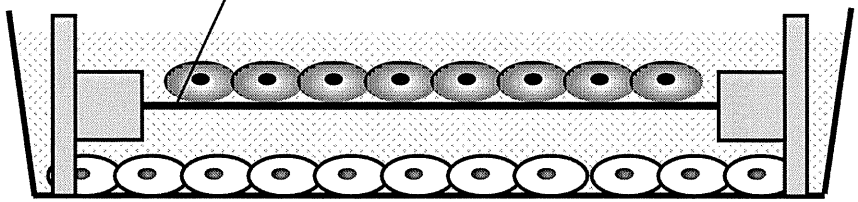

Separate co-culture (SC)

(B)

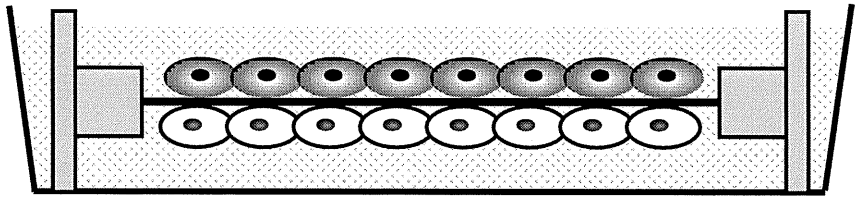

Sandwich co-culture (SW)

506

Rat dental epithelial cell line (HAT-7)

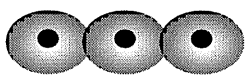

Bovine dental folicle cell line (BCPb8)

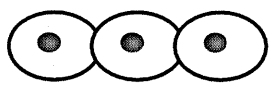

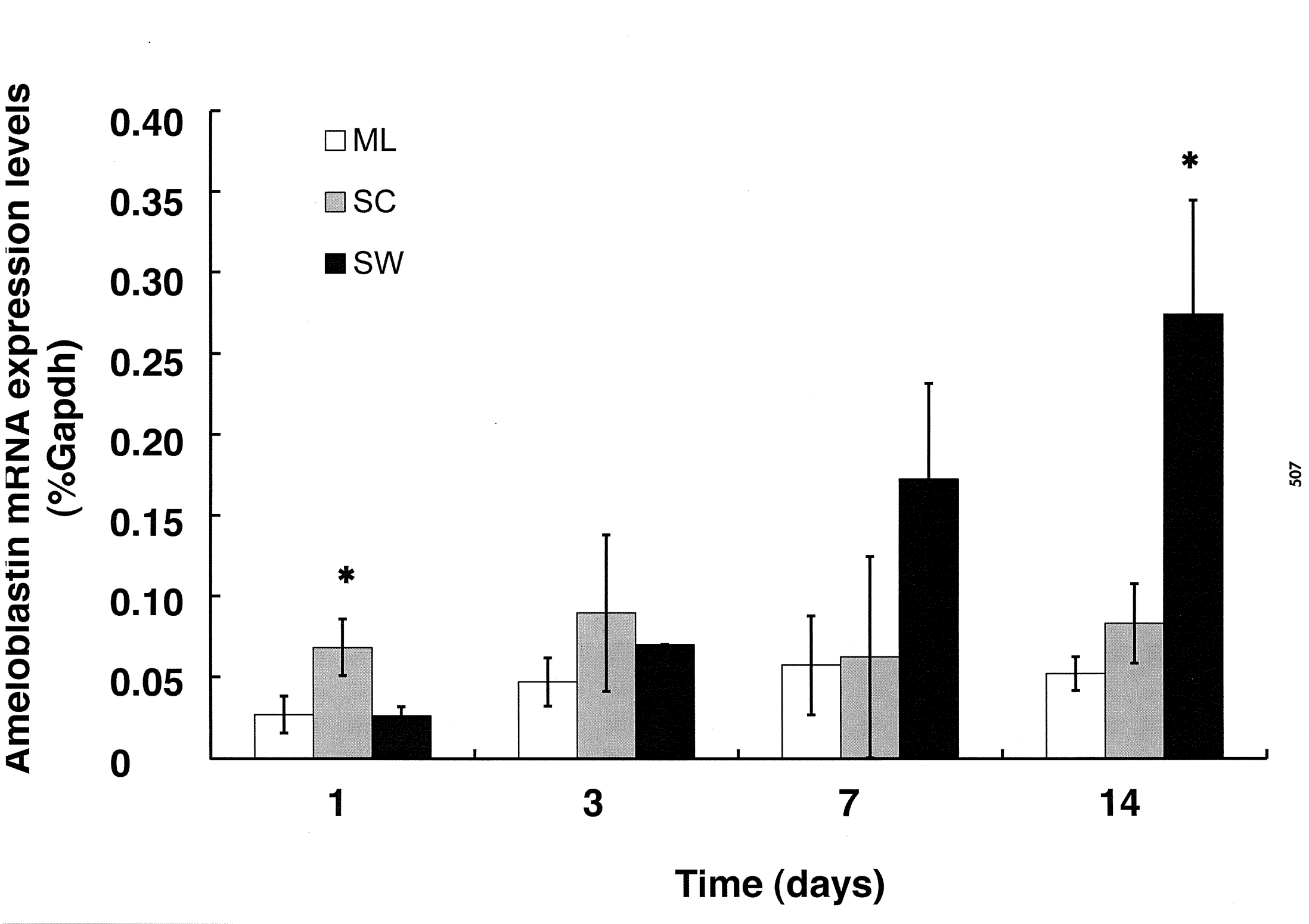
Ameloblastin mRNA expression levels
(%Gapdh)
0.40
0.35
0.30
0.25
0.20
0.15
0.10
0.05
0
ML
SC
SW
*
*
1
3
7
14
Time (days)
507

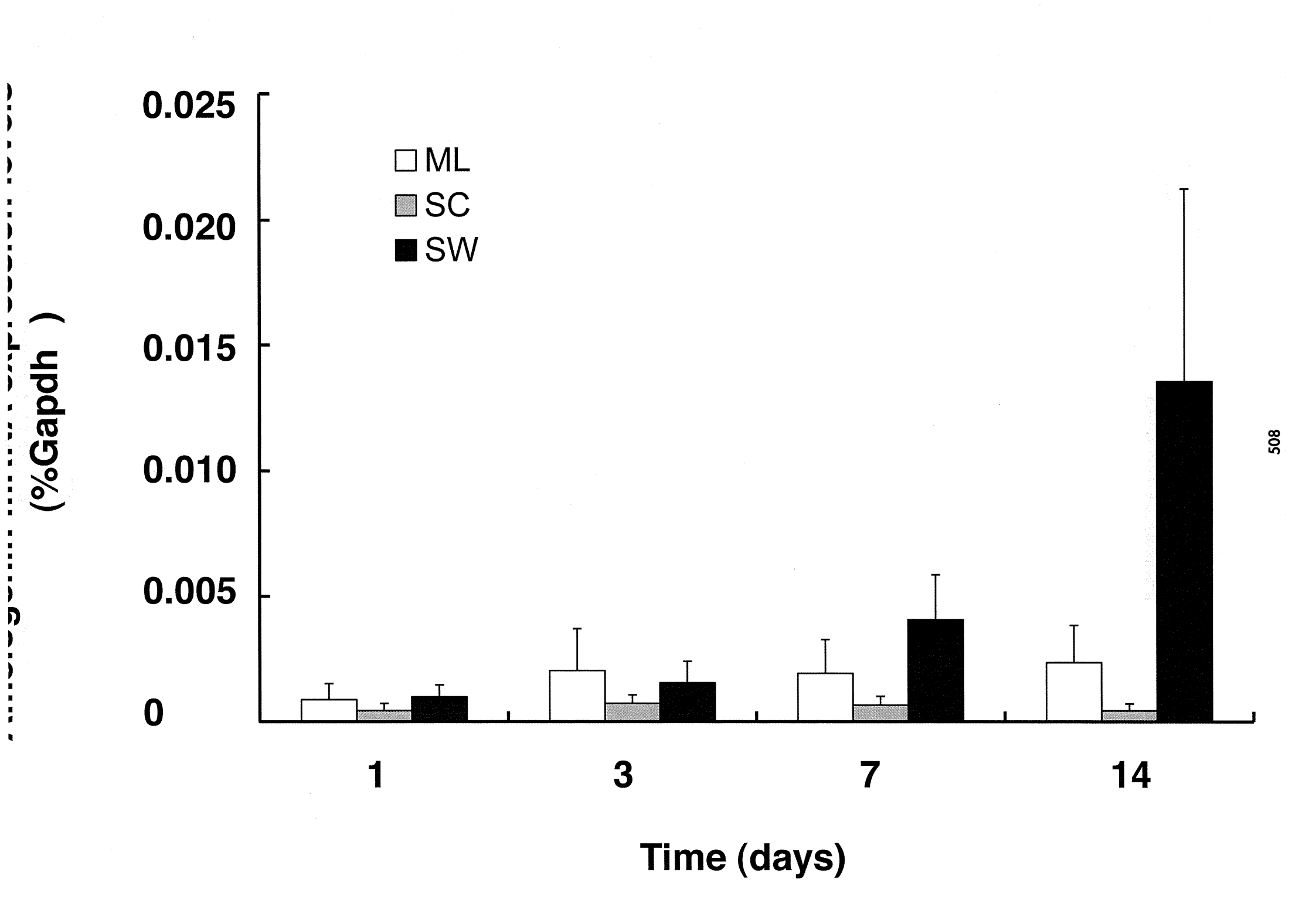
0.025
0.020
0.015
0.010
0.005
0
(%Gapdh)
ML
SC
SW
1
3
7
14
Time (days)
508

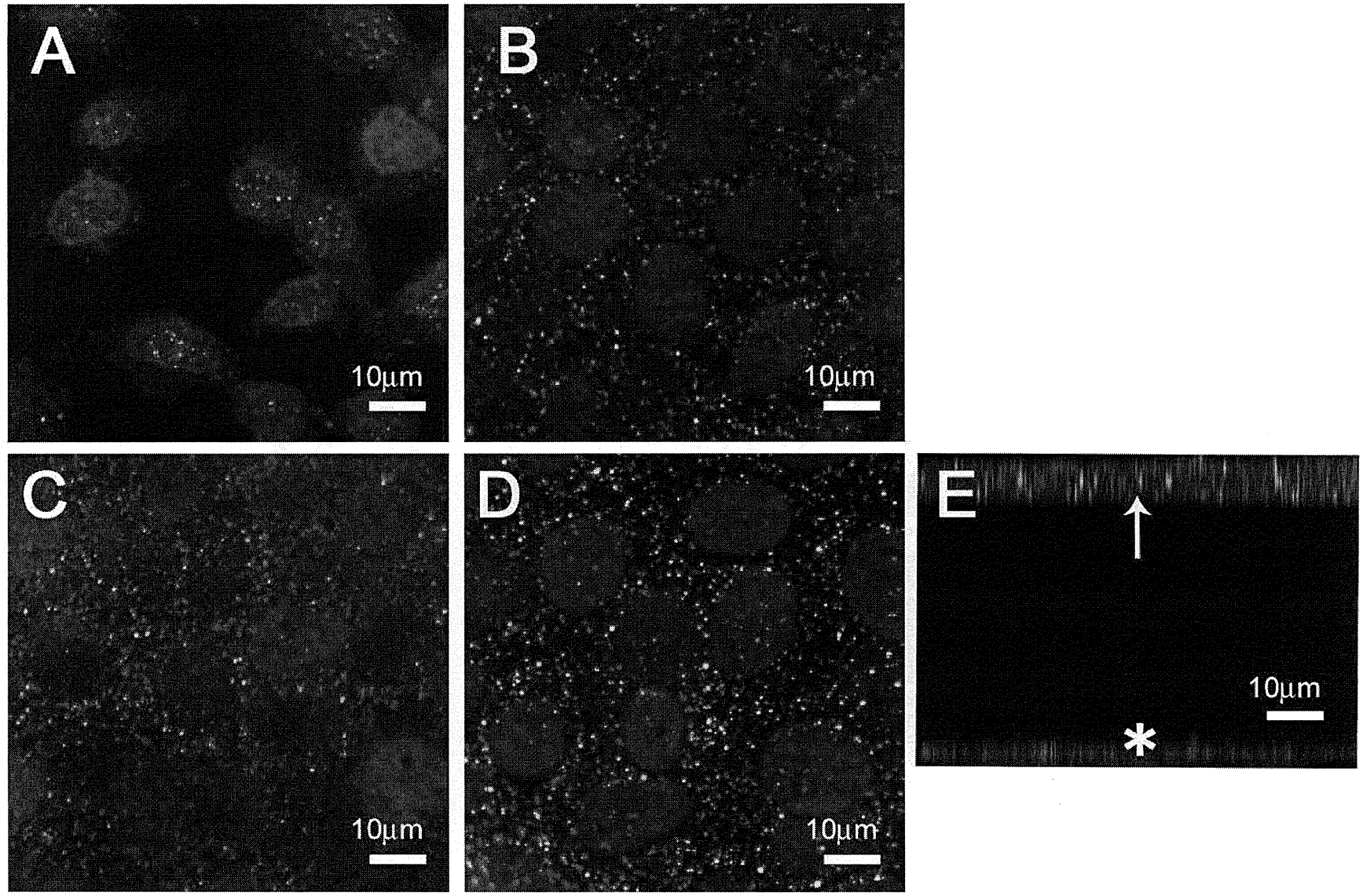

509

Fig.4 by Matsumoto et a

Cell Tissue Res (2010) 341:381–395
DOI 10.1007/s00441-010-1021-5

REGULAR ARTICLE

Dilated capillaries, disorganized collagen fibers and differential gene expression in periodontal ligaments of hypomorphic fibrillin-1 mice

Ganjargal Ganburged · Naoto Suda · Masahiro Saito · Yosuke Yamazaki · Keitaro Isokawa · Keiji Moriyama

Received: 18 December 2009 / Accepted: 13 July 2010 / Published online: 17 August 2010

Abstract The periodontal ligaments (PDLs) are soft connective tissue between the cementum covering the tooth root surface and alveolar bone. PDLs are composed of collagen and elastic system fibers, blood vessels, nerves, and various types of cells. Elastic system fibers are generally formed by elastin and microfibrils, but PDLs are mainly composed of the latter. Compared with the well-known function of collagen fibers to support teeth, little is known about the role of elastic system fibers in PDLs. To clarify their role, we examined PDLs of mice under-expressing fibrillin-1 (mgR mice), which is one of the major microfibrillar proteins. The PDLs of homozygous mgR mice showed one-quarter of the elastic system fibers of wild-type (WT) mice. A close association between the elastic system fibers and the capillaries was noted in WT, homozygous and heterozygous mgR mice. Interestingly, capillaries in PDLs of homozygous mice were dilated or enlarged compared with those of WT mice. A comparable level of type I collagen, which is the major collagen in PDLs, was expressed in PDL-cells of mice with three genotypes. However, multi-oriented collagen fiber bundles with a thinner appearance were noted in homozygous mice, whereas well-organized collagen fiber bundles were seen in WT mice. Moreover, there was a marked decrease in periostin expression, which is known to regulate the fibrillogenesis and crosslinking of collagen. These observations suggest that the microfibrillar protein, fibrillin-1, is indispensable for normal tissue architecture and gene expression of PDLs.

Keywords Fibrillin-1 · Periodontal ligament · Periostin · Type I collagen · Sharpey's fibers · Mouse (mgR)

Funding This study was supported by Grant-in-Aid for Scientific Research from the Ministry of Education, Culture, Sports, Science, and Technology of Japan (No. 18390552, 19659547, and 21390546), by Sato Fund and Dental Research Center Grant at Nihon University School of Dentistry, and by Grant for Supporting Project for Strategic Research of Nihon University School Dentistry at Matsudo by the Ministry of Education, Culture, Sports, Science, and Technology of Japan.

G. Ganburged · N. Suda (✉) · K. Moriyama
Maxillofacial Orthognathics, Department of Maxillofacial Reconstruction and Function, Division of Maxillofacial/Neck Reconstruction, Graduate School of Medical and Dental Sciences, Tokyo Medical and Dental University,
1-5-45 Yushima, Bunkyo-ku,
Tokyo 113-8510, Japan
e-mail: n-suda.mort@tmd.ac.jp

G. Ganburged · N. Suda · K. Moriyama
Global Center of Excellence (GCOE) Program, International Research Center for Molecular Science in Tooth and Bone Diseases,
Tokyo, Japan

M. Saito
Research Institute for Science and Technology, Tokyo University of Science,
Chiba, Japan

Y. Yamazaki · K. Isokawa
Department of Anatomy, Nihon University School of Dentistry,
Tokyo, Japan

Y. Yamazaki · K. Isokawa
Division of Functional Morphology, Dental Research Center, Nihon University School of Dentistry,
Tokyo, Japan

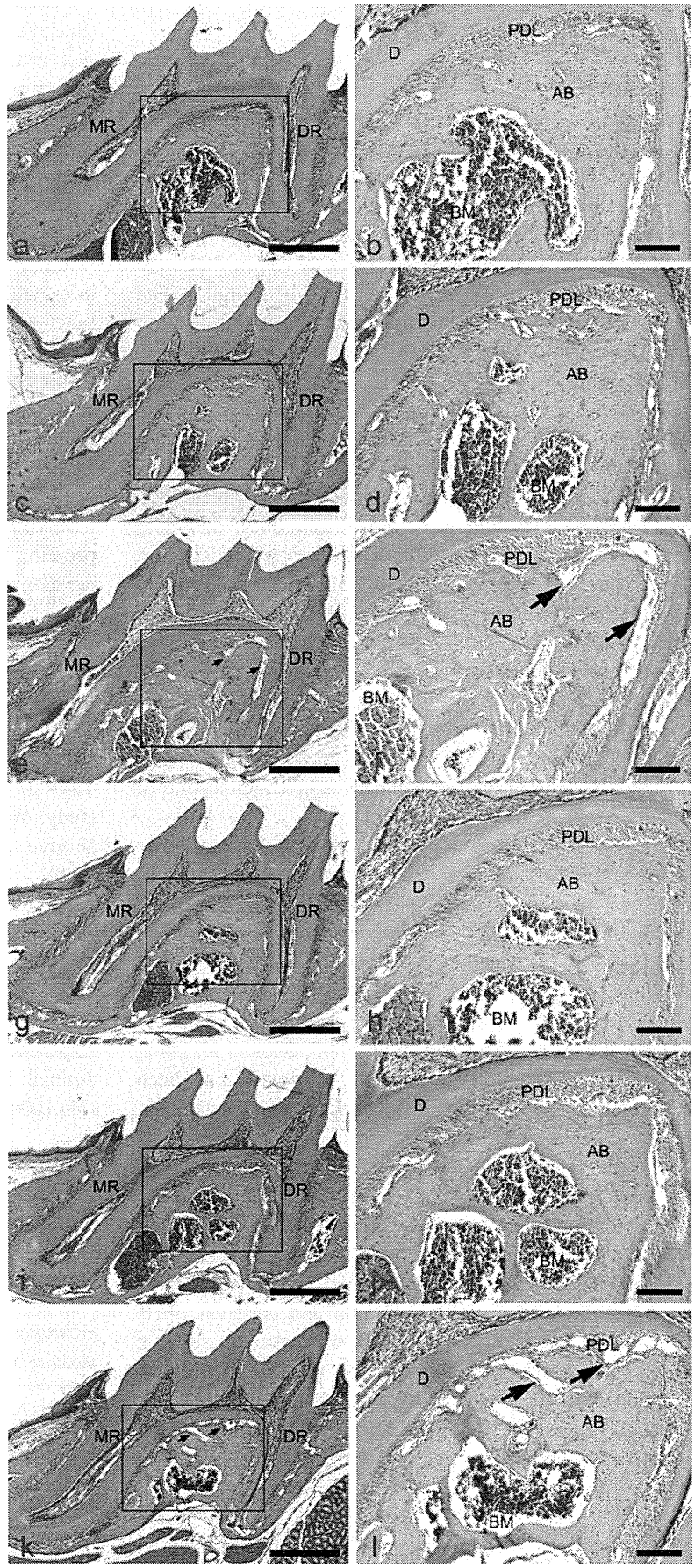

Fig. 1 Histological appearance of hematoxylin and eosin-stained sections around maxillary first molars in 2- (**a**–**f**) and 8-week-old (**g**–**l**) mice. WT (**a**,**b**,**g**,**h**), heterozygous (**c**,**d**,**i**,**j**), and homozygous (**e**,**f**,**k**,**l**) mice are shown. Higher magnifications of *boxed areas* in (**a**,**c**,**e**,**g**,**i**,**k**) are shown in (**b**,**d**,**f**,**h**,**j**, **l**), respectively. Note that many capillaries were present in the PDLs, and dilated capillaries (*arrows* in **e**,**f**,**k**,**l**) were noted in the homozygous mice but not in the other types of mice. This was more apparent in 8-week-old homozygous mice compared with those at 2 weeks. Magnification ×4 (**a**,**c**,**e**,**g**,**i**,**k**),× 10 (**b**,**d**,**f**, **h**,**j**,**l**). *AB* Alveolar bone, *BM* bone marrow, *D* dentin, *DR* distal root, *MR* mesial root, *PDL* periodontal ligament. *Bars* 400 μm (**a**,**c**,**e**,**g**,**i**,**k**), 100 μm (**b**,**d**,**f**,**h**,**j**,**l**)

Introduction

Periodontal ligaments (PDLs) are characteristic and specialized connective tissue, located between the socket of the alveolar bone and cementum covering tooth roots (Nanci 2007). PDLs are composed of fibers, blood vessels, nerves, and various kinds of cells. More than half of these structural elements are collagen fibers (Freezer and Sims 1987). Most of the collagen fibrils in PDLs are arranged in definite and well-organized fiber bundles. The termini of collagen fiber bundles of PDLs are at the end of the alveolar bone and cementum, and are termed as Sharpey's fibers.

The predominant collagens of PDLs are types I, III and XII. Among them, type I is the most abundant (Nanci 2007) and its expression becomes apparent in PDLs as root forms (MacNeil et al. 1998). Type XII collagen is seen in a relatively large amount in ligamentous tissues, including PDLs (Karimbux et al. 1992; Karimbux and Nishimura 1995; MacNeil et al. 1998). Type XII collagen belongs to the Fibril Associated Collagens with Interrupted Triple Helices (FACITs), having short triple-helical domains separated by non-triple-helical regions (Gordon et al. 1987; Shaw and Olsen 1991). A study of transgenic mice carrying a dominant interference mutation in type XII collagen [truncated α1 (XII)] indicated that this collagen plays an important role in the extracellular matrix architecture of PDLs (Reichenberger et al. 2000).

Periostin was originally termed osteoblast-specific factor-2 (Osf-2), and is known to exhibit structural similarity to a homophilic adhesion molecule, fasciclin-1 (Takeshita et al. 1993). This molecule is predominantly expressed in collagen-rich fibrous connective tissues. Periostin is expressed in PDLs, and accumulating evidence suggests that this molecule is required to maintain the integrity of PDLs (Afanador et al. 2005; Rios et al. 2005, 2008; Kii et al. 2006). Recently, periostin has been suggested to regulate the fibrillogenesis and crosslinking of collagens (Norris et al. 2007).

Elastic system fibers are widely distributed among various types of connective tissue where elasticity is required, such as the skin, lung, and blood vessels (Mecham 1991). These fibers are composed of elastin and microfibrils. Depending on the relative amount of elastin, they are classified as elastic, elaunin and oxytalan fibers (Kielty et al. 2002). Oxytalan fibers, which lack elastin, are made up of bundles of 10- to 12-nm microfibrils that are predominantly composed of glycoproteins, fibrillin-1 and -2. In PDLs, the main elastic system fibers are oxytalan fibers, which are oriented in an occluso-apical direction (Fullmer et al. 1974; Beertsen et al. 1997; Tashiro et al. 2002; Shiga et al. 2008; Suda et al. 2009; Tsuruga et al. 2009). There is also a small amount of elaunin fibers in the apical region (Staszyk and Gasse 2004; Sawada et al. 2006). It is known that mutation in the gene encoding fibrillin-1, *FBN1*, causes an autosomal dominant disorder Marfan syndrome type I (MFS1, MIM #154700), characterized by tall stature, aortic dissection, mitral valve prolapse and ectopia lentis (Pyeritz 2000). In addition to these conditions, severe periodontitis is frequently associated with this syndrome (De Coster et al. 2002)

Compared with collagen fibers, there is only limited information on elastic system fibers in PDLs. To clarify the function of elastic system fibers in PDLs, we examined PDLs in hypomorphic fibrillin-1 mice (mgR), which showed the reduction of *Fbn1* (encoding mouse fibrillin-1) expression as a result of transcriptional interference by insertion of the PGK*neo*-cassette (Pereira et al. 1999). Findings in this study showed the aberrant architecture of collagen fibers and differential gene expression of PDL-cells in mgR mice, suggesting that the microfibrillar protein, fibrillin-1, is indispensable for normal PDL development.

Materials and methods

Animals

Two- to eight-week-old male mgR mice were used in this study. We found that homozygous mgR mice could only survive for up to 3 or 4 months, as reported (Pereira et al. 1999). Thus, heterozygous mgR mice were mated to generate wild-type (WT), heterozygous, and homozygous mgR mice. Totals of 16 WT (6 at 2 weeks; 4 at 6 weeks; 6 at 8 weeks), 16 heterozygous (6 at 2 weeks; 4 at 6 weeks; 6 at 8 weeks), and 15 homozygous mgR (6 at 2 weeks; 3 at 6 weeks; 6 at 8 weeks) mice were used in this study. Experimental procedures were approved by the Experimental Animal Committee of Tokyo Medical and Dental University (No.100073).

Table 1 The sum of the capillary size in PDLs of WT, heterozygous and homozygous mgR mice

Genotype of mice	Mean	SE	*P* value
WT mice	976.8	172.1	-
Heterozygous mgR mice	2,010.4	228.4	<0.01[a]
Homozygous mgR mice	2,892.5	231.9	<0.001[b]

Each value is represented as μm^2. The mean and SE values were calculated from six different sections in each kind of genotype, as described in "Materials and methods". Eight-week-old mice were used for the evaluation

[a] WT versus heterozygous mgR mice

[b] WT versus homozygous mgR mice

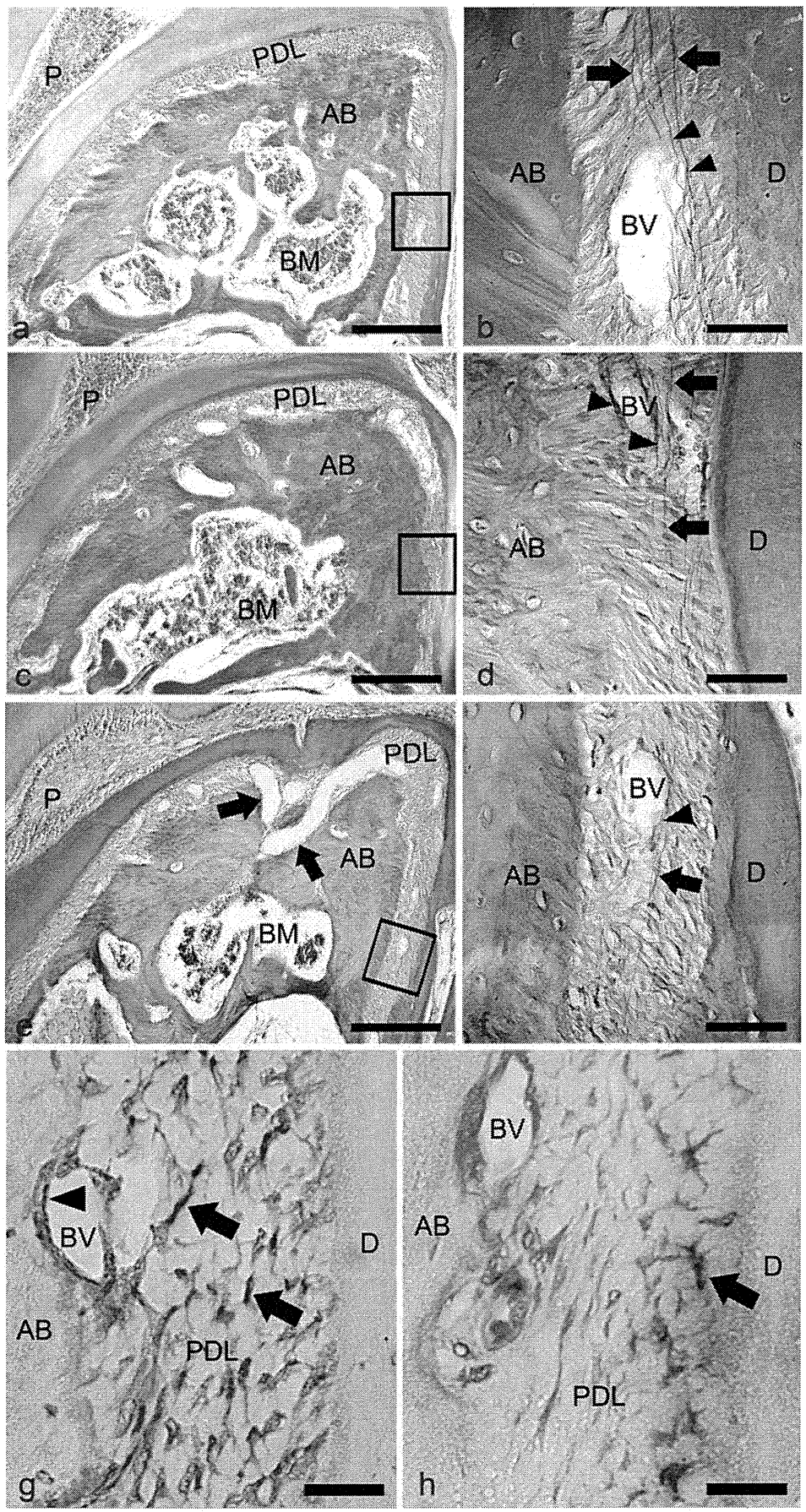

Fig. 2 Resorcin-Fuschin stained sections showing elastic system fibers around maxillary first molars of WT (**a**,**b**), heterozygous (**c**,**d**), and homozygous (**e**,**f**) mice at 2 weeks of age. Higher magnifications of *boxed areas* in (**a**,**c**,**e**) are shown in (**b**, **d**,**f**), respectively. Stained fibers (*arrows* in **b**,**d**) were clearly seen, and there was an association between the stained fibers and capillaries (*arrowheads* in **b**,**d**) in the WT and heterozygous mice. A lower amounts of elastic system fibers with a shorter appearance (*arrow* in **f**) were noted in the homozygous mice. Also, there were lower amounts of fibers showing an association with the capillaries (*arrowhead* in **f**) in the homozygous mice. Some dilated capillaries were noted in homozygous mice (*arrows* in **e**). In situ hybridization of fibrillin-1 in the PDLs of WT (**g**) and homozygous (**h**) mice. The expression was clearly seen in PDL-cells (*arrows* in **g**,**h**) of both genotypes, and there were lower numbers of fibrillin-1 expressing cells in homozygous mice than in WT mice. The expression was seen in endothelial cells (*arrowhead*) in WT mice but not in homozygous mice. Magnification× 10 (**a**,**c**,**e**), ×40 (**b**,**d**,**f**), ×60 (**g**,**h**). *AB* Alveolar bone, *BM* bone marrow, *BV* capillaries, *D* dentin, *PDL* periodontal ligament, *P* dental pulp. *Bars* 200 μm (**a**,**c**,**e**), 40 μm (**b**,**d**,**f**), 25 μm (**g**,**h**)

Table 2 Resorcin-fuchsin stained areas in PDLs of WT, heterozygous and homozygous mgR mice

Genotype of mice	Mean	SE	*P* value
WT mice	22.34	2.69	-
Heterozygous mgR mice	10.39	1.29	<0.001[a]
Homozygous mgR mice	5.33	0.70	<0.001[b]

Each value is represented as $\mu m^2/mm^2$. The mean and SE values were calculated from 18 different Resorcin-fuchsin stained areas in each kind of genotype, as described in "Materials and methods". Six-week-old mice were used for the evaluation

[a] WT versus heterozygous mgR mice

[b] WT versus homozygous mgR mice

Histological preparation

Mice were anesthetized with 50 mg/ml sodium pentobarbital and perfusion fixation was performed using 4% paraformaldehyde in 0.1 M phosphate buffer (PBS, pH 7.4) treated with diethylpyrocarbonate (DEPC). Maxillae were dissected and decalcified in Morse solution (10% sodium citrate, 20% formic acid, Wako, Japan) for one week, and dehydrated and embedded in paraffin (Wako). Five-μm-thick serial sagittal sections of the maxillary molars with surrounding tissue were prepared for light-microscopic observation. Some sections were deparaffinized and stained by hematoxylin (Muto Pure Chemicals, Japan) and 0.5% eosin Y ethanol (Wako) solution.

To visualize the elastic system fibers, sections were stained by Resorcin-fuchsin solution (Muto Pure Chemicals) after 10% oxone (Wako) treatment and counterstained by 1% Orange G (Wako). With oxone treatment, both elastin and microfibrils can be visualized.

Picrosirius polarization staining

To highlight collagen fibers in PDLs, sections were stained with Picrosirius red solution (Muto Pure Chemicals) and washed in 0.005% acetic acid solution before mounting on cover slides. Collagen orientation was observed three dimensionally, using a polarizing light microscope (Eclipse LV100 POL; Nikon, Japan). Details of collagen orientation have been described by Rieppo et al. (2008).

In situ hybridization

Both the sense and antisense digoxigenin-11-uridine triphosphate (DIG-11-UTP)-labeled single-stranded RNA probes of *Col12a1* (encoding mouse type XII collagen), *Fbn1* (encoding mouse fibrillin-1), and *postn* (encoding mouse periostin) were prepared using a DIG RNA labeling kit (Roche, Indianapolis, IN, USA) according to the manufacturer's instructions. The template cDNA was a 503-bp *Spe* I-*Not* I fragment of *Col12a1* (corresponding to 7152-7654 in NM_007730), a 522-bp *Spe* I-*Not* I fragment of *Postn* (corresponding to 11-532 in NM_015784), and a 500-bp *Spe* I-*Not* I fragment of *Fbn1* (corresponding to 6952-7451 in NM_007993). The template cDNA of *Col1a1* (encoding mouse type I collagen) was cloned by reversed transcription-PCR, according to the website of the Allen Institute for Brain Science (http://mouse.brain-map.org/brain/Col1a1/71992079.html?ispopup=true), and labeled by a DIG RNA labeling kit. The hybridization procedure was carried out as previously described (Suda et al. 2001). Briefly, deparaffinized sections were treated with proteinase K at 37°C, followed by hybridization with a DIG-labeled probe for 16 h at 60°C. After hybridization, slides were washed to remove unbound probes. The DIG-labeled probes were detected using a nucleic acid detection kit (Roche) according to the manufacturer's instructions. Sections were counterstained with 0.5% eosin Y ethanol solution (Wako).

Immunostaining

Immunostaining of von Willebrand factor (ADAMTS13) was performed by using the rabbit polyclonal antibody against human von Willebrand factor (Novus Biologicals, Littleton, CO, USA). The goat anti-rabbit IgG antibody conjugated to horseradish peroxidase (HRP) (Novus Biologicals) was used as a second antibody, and a color detection was performed by using diaminobenzidine (DAB). Immunostaining of PECAM-1 (CD31) was performed by using the rat monoclonal antibody against mouse PECAM-1 (Santa Cruz Biotechnology, Santa Cruz, CA, USA) and the rat ABC staining system (Santa Cruz Biotechnology), according to the manufacturer's instruction. All sections were counterstained with 0.05% toluidine blue solution and visualized under light microscopy.

Apoptotic cells in PDLs

To examine the TUNEL (TdT-mediated dUTP-biotin nick end labeling)-positive apoptotic cells around capillaries in PDLs, in situ cell death detection kit (Roche) was used, according to the manufacturer's instruction.

Electron-microscopic observation

Ultrathin sections of 6-week-old mice were prepared from embedded (Epon 812; TAAB, England) specimens. Sections were prepared from an identical level of each root (at the middle of each root length). The sections were contrasted with 2.5% uranyl acetate and Sato's lead salts (Sato 1968), and examined with a transmission

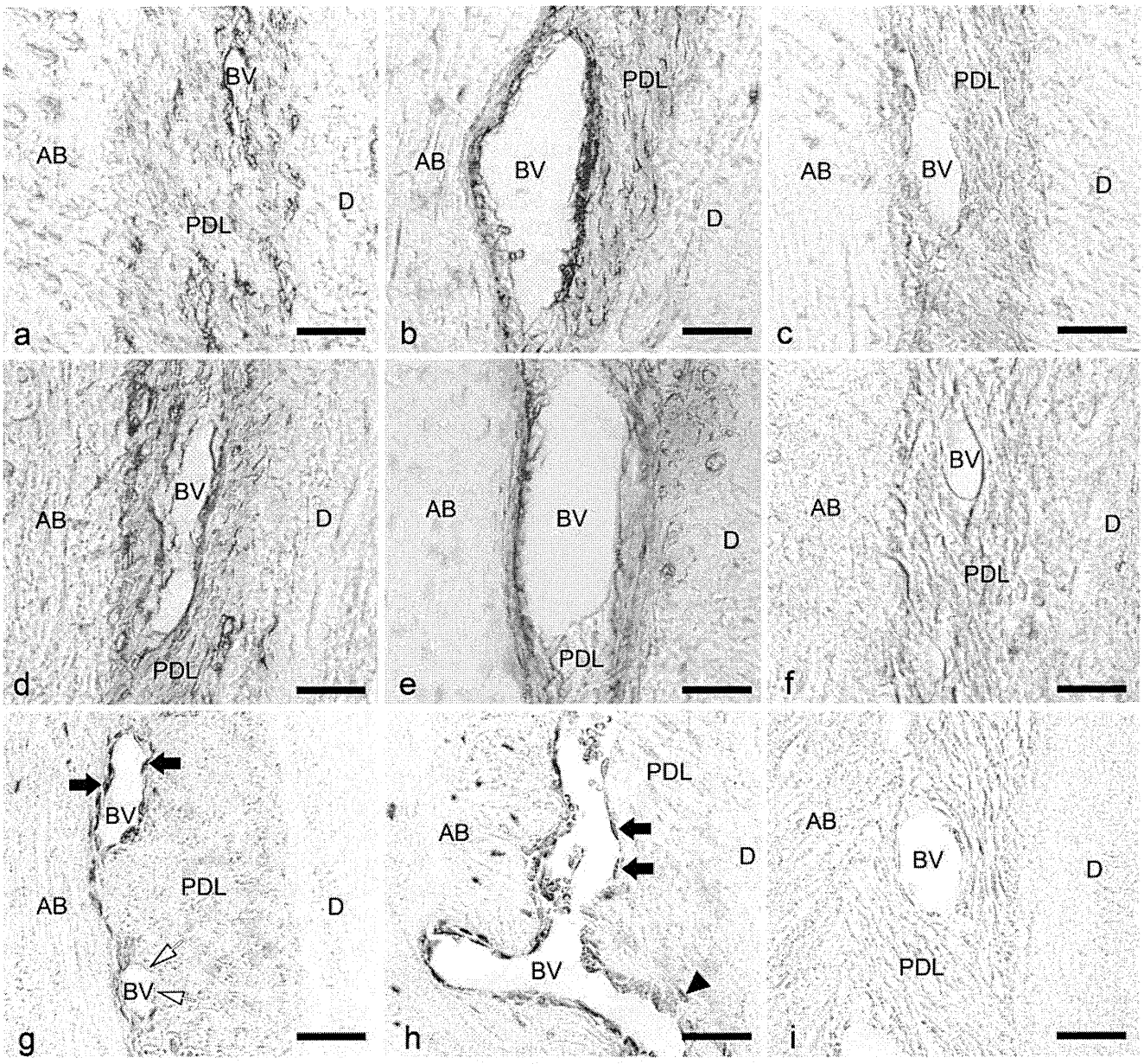

Fig. 3 Immunolocalization of PECAM-1 (CD31) (**a**–**c**) and von Willebrand factor (**d**–**f**) in the PDLs of 8-week-old mice. Sections of WT (**a**,**c**,**d**,**f**) and homozygous (**b**,**e**) mice. The immunoreaction of PECAM-1 and von Willebrand factor was seen in endothelial cells of WT (**a**,**d**) and homozygous mgR mice (**b**,**e**). The negative controls, in which the rabbit polyclonal antibody against von Willebrand factor was replaced with the normal rabbit serum (**c**), and the rat monoclonal antibody against mouse PECAM-1 was replaced with the rat Ig (**f**), are shown. The TUNEL-staining of the PDLs in WT (**g**,**i**) and homozygous mice (**h**) at 8 weeks of age. The section of WT mouse without using the terminal deoxynucleotidyl transferase is shown in (**i**). TUNEL-positive cells were seen around capillaries in both WT (**g**) and homozygous mice (**h**). There were larger numbers of TUNEL-positive cells around capillaries of homozygous mice than in WT mice. Magnification ×40; *black arrows* TUNEL-positive endothelial cells, *white arrows* TUNEL-negative endothelial cells, *arrowhead* fibroblastic cell, *AB* alveolar bone, *BV* capillaries, *D* dentin, PDL periodontal ligament. *Bars* 20 μm

electron microscope (H-800; Hitachi, Tokyo, Japan) at an accelerating voltage of 75 kV.

Statistical analysis

To compare the capillary size of PDLs in WT, heterozygous and homozygous mgR, sagittal sections (7-μm-thick) were prepared from the maxillary first molars of each 8-week-old mouse. Three mice were used for each genotype. Two sections were prepared from the middle of the buccal and lingual dimension of each tooth root. The sum of the capillary sizes were evaluated in two unoverlapped rectangular areas in PDLs (two 750 μm×100 μm rectangular areas in the bifurcation and in the mesial

Table 3 The number of TUNEL- positive cells around capillaries in PDLs

Genotype of mice	Mean	SE	*P* value
WT mice	0.43	0.06	
Homozygous mgR mice	1.12	0.11	< 0.001[a]

Each value is represented as cells/mm^2. The mean and SE values were calculated around 24 different capillaries in each genotype, as described in "Materials and methods". Eight-week-old mice were used for the evaluation

[a] WT versus homozygous mgR mice

side of the distal root, in each section). The ANOVA and Fisher's PLSD test were used to examine the differences between the WT, heterozygous, and homozygous mgR mice.

To compare the amount of elastic system fibers in WT, heterozygous and homozygous mgR mice, cross sections (7-μm-thick) of the distal sides of the distal roots were prepared from the maxillary first molars of each 6-week-old mouse. Three mice were used for each genotype. Two sections were prepared from an identical level of each root (at the middle of each root length) and stained by Resorcin-fuchsin solution with oxone pretreatment. Stained areas were evaluated in three randomly chosen areas in each section. A total of 18 areas were used for each genotype. ImageJ (ver.1.4.3; National Institutes of Health, MD, USA) was used for measuring Resorcin-fuchsin stained areas. The ANOVA and Steel-Dwass test were used to examine the differences between WT, heterozygous, and homozygous mgR mice.

To compare the number of apoptotic cells around capillaries in PDLs between WT and homozygous mgR mice. Four mice were used for each genotype. Two sections were prepared from the middle of the buccal and lingual dimension of the maxillary first molars in each 8-week-old mouse. Three capillaries were randomly chosen in the mesial side of the distal root in each section. A total of 24 capillaries were used for each genotype. The number of TUNEL-positive cells were counted in areas within 5 μm from each capillary. The Student's *t* test was used to examine the difference in the cell numbers between the WT and homozygous mgR mice. All statistical analyses were carried out with R (ver.2.10.0; R Foundation for Statistical Computing, Austria). *P* values less than 0.05 were considered significant.

Results

The histological appearances of the upper first molars and periodontal tissues of WT, heterozygous, and homozygous mgR mice are shown in Fig. 1. The appearance of the crown and root shape did not differ among the mice with three genotypes at 2 (Fig. 1a–f) or 8 (Fig. 1g–l) weeks old. A comparable thickness of PDLs was seen in mice with three genotypes, and bone marrows were similarly under the bifurcation areas (Fig. 1b, d, f, h, j, l). In both 2- and 8-week-old mice, numerous capillaries were seen in the PDLs. Dilated capillaries were noted in homozygous mice (Fig. 1f, l) but not in the other two types of mice. This was more apparent in 8-week-old homozygous mice (Fig. 1l) compared with those at 2 weeks old (Fig. 1f). The quantitative analysis of capillaries in the PDLs showed that the sum of capillary sizes in the heterozygous (2,010.4 μm^2) and homozygous (2,892.5 μm^2) mgR mice were significantly larger than that of WT mice (976.8 μm^2) (Table 1).

To highlight the elastic system fibers in PDLs, Resorcin-fuchsin staining was performed in 2-week-old mice with the three genotypes (Fig. 2). Fibers positive for this staining ran vertically in the PDLs of the three types of mice (Fig. 2b, d, f). There were many linear staining patterns in the WT and heterozygous mgR mice, and an association between elastic system fibers and capillaries was noted (Fig. 2b, d). In homozygous mice, there was a marked decrease in the amount of elastic system fibers, and fibers were shorter than those in WT and heterozygous mice (Fig. 2f). Additionally, there were fewer fibers showing an association to capillaries in homozygous mice than in the other two types of mice. All these stainings were performed by oxone treatment to visualize both elastin and microfibrils. Without oxone treatment, it is known that elastin but not microfibrils can be stained (Fullmer et al. 1974). PDLs were minimally stained without oxone treatment (data not shown), indicating that the majority of elastic system fibers in the mouse PDLs were microfibrils. Quantitative analysis of the amount of elastic system fibers in PDLs showed that there was a significant reduction in heterozygous (53.5% reduction to 10.39 μm^2/mm^2) and homozygous (76.1% reduction to 5.33 μm^2/mm^2) mice, compared to WT mice (22.34 μm^2/mm^2) (Table 2). In situ hybridization was performed to examine mRNA expression of fibrillin-1 in PDLs of the WT (Fig. 2g) and homozygous mgR (Fig. 2h) mice. The expression was clearly seen in PDL-cells of both genotypes, but there were lower numbers of fibrillin-1 expressing cells in homozygous mice than in WT mice. As reported in human endothelial cells (Vehviläinen et al. 2009), the expression was seen in endothelial cells of WT mice (Fig. 2g). But it was scarcely seen in endothelial cells of homozygous mgR mice (Fig. 2h).

Endothelial cells were immunostained by using specific antibodies against PECAM-1 (CD31) and von Willebrand factor (Fig. 3). The observation showed that immuno-reaction against these antibodies was clearly seen in the

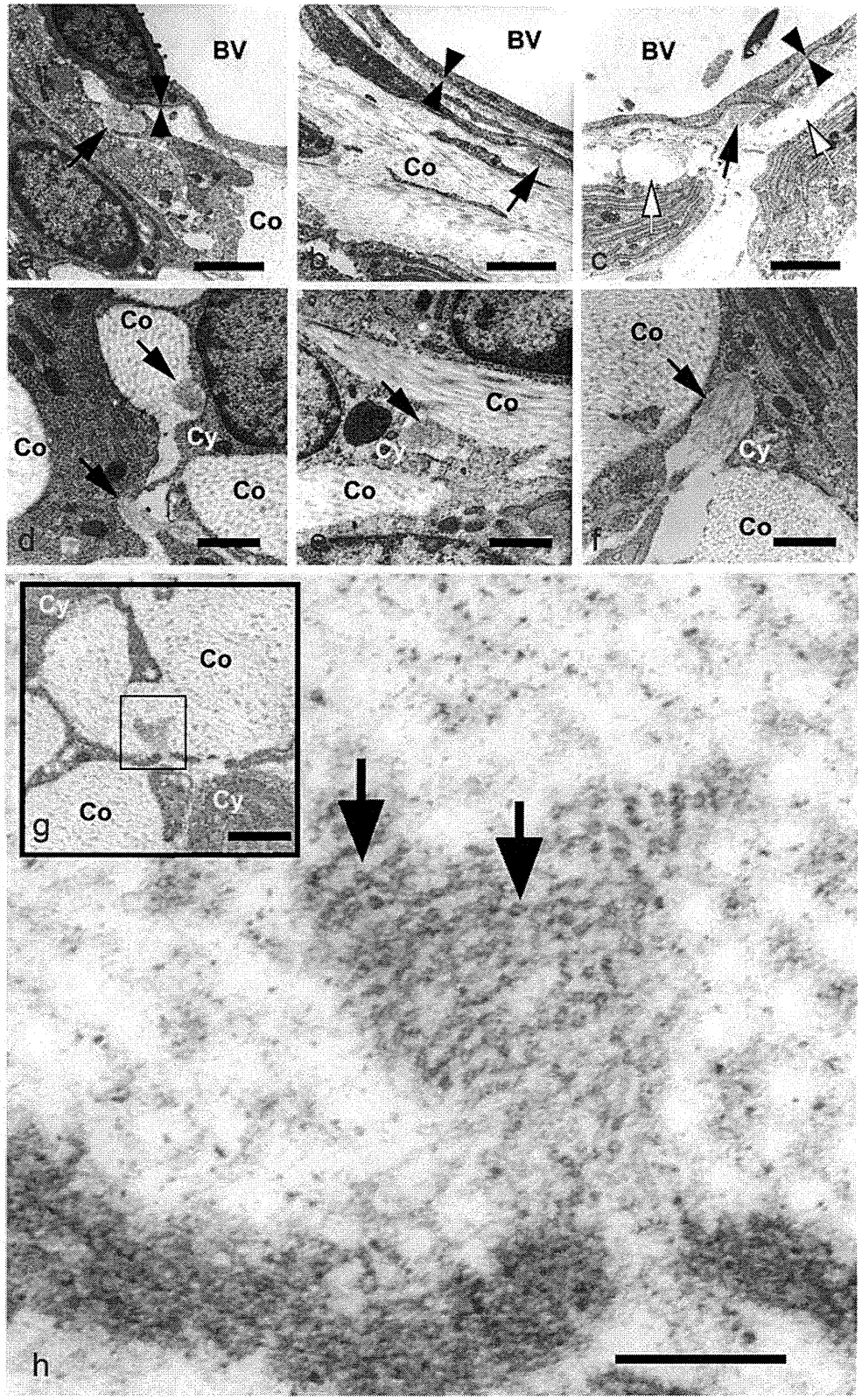

Fig. 4 Electron-microscopic observation of the PDLs of WT (**a**,**d**,**g**,**h**), heterozygous (**b**,**e**), and homozygous (**c**,**f**) mice. Sections around (**a**–**c**) and not around (**d**–**h**) the capillaries (*BV*) are shown. Bundles of microfibrils (*black arrows* in **a**–**f**,**h**) lacked any apparent amorphous appearance of elastin deposition and showed tubular structure (*black arrows* in **h**), indicating that there were elastin-free microfibrils. Note that each bundle of microfibrils (*black arrows* in **d**–**f**) was exclusively located adjacent to the PDL-cells and seen between the cytoplasmic processes. Degenerative cells (*white arrows* in **c**) were noted around capillaries in the homozygous mice, but scarcely seen in the heterozygous and never seen in the WT mice, respectively. Microfibrils were seen close to the basement membranes (*double arrowheads* in **a**–**c**). The *boxed area* in **g** is shown at higher magnification in **h**. *Co* Collagen, *Cy* cytoplasmic process. Magnification×10,000 (**a**–**c**),× 18,000 (**d**–**g**),×54,000 (**h**). *Bars* 5 nm (**a**–**c**), 2.5 nm (**d**–**g**), 0.5 nm (**h**)

endothelial cells of WT (Fig. 3a, d) and homozygous mgR mice (Fig. 3b, e). There were no stained cells in negative controls in which specific primary antibodies did not react (Fig. 3c, f). Next, apoptotic cells were examined by TUNEL staining (Fig. 3g–i). The TUNEL-positive cells were seen around capillaries both in the WT (Fig. 3g) and homozygous mgR mice (Fig. 3h). The endothelial cells in WT mice were both positive and negative to TUNEL